JACS
JOURNAL OF THE AMERICAN CHEMICAL SOCIETY
Article
pubs.acs.org/JACS

Multivariate Metal–Organic Frameworks for Dialing-in the Binding and Programming the Release of Drug Molecules

Zhiyue Dong,[†] Yangzesheng Sun,[†] Jun Chu,[†] Xianzheng Zhang,[†,‡] and Hexiang Deng*[,†,‡]

[†]Key Laboratory of Biomedical Polymers-Ministry of Education, College of Chemistry and Molecular Sciences, and [‡]UC Berkeley-Wuhan University Joint Innovative Center, The Institute of Advanced Studies, Wuhan University, Luojiashan, Wuhan 430072, China

Supporting Information

ABSTRACT: We report the control of guest release profiles by dialing-in desirable interactions between guest molecules and pores in metal–organic frameworks (MOFs). The interactions can be derived by the rate constants that were quantitatively correlated with the type of functional group and its proportion in the porous structure; thus the release of guest molecules can be predicted and programmed. Specifically, three probe molecules (ibuprofen, rhodamine B, and doxorubicin) were studied in a series of robust and mesoporous MOFs with multiple functional groups [MIL-101(Fe)-$(NH_2)_x$, MIL-101(Fe)-$(C_4H_4)_x$, and MIL-101(Fe)-$(C_4H_4)_x(NH_2)_{1-x}$]. The release rate can be adjusted by 32-fold [rhodamine from MIL-101(Fe)-$(NH_2)_x$], and the time of release peak can be shifted by up to 12 days over a 40-day release period [doxorubicin from MIL-101(Fe)-$(C_4H_4)_x(NH_2)_{1-x}$], which was not obtained in the physical mixture of the single component MOF counterparts nor in other porous materials. The corelease of two pro-drug molecules (ibuprofen and doxorubicin) was also achieved.

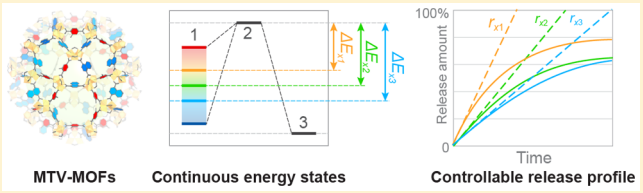

INTRODUCTION

One of the most important properties of porous crystalline materials is their ability to bind molecules in a specific manner on the basis of the host–guest interactions taking place within the pores. This is epitomized in the chemistry of discrete molecular systems and extended frameworks,[1] where the pores can be chemically and geometrically modified to selectively bind a target guest molecule, and to direct its uptake and release behavior. Although host–guest interactions have been designed and studied extensively,[2] the ability to dial-in a desired interaction and thus precisely program the release of guests in porous systems remains largely undeveloped. The reason for this is that simple variation of functional groups can only allow the pores to access a few discrete energy states engendered by the host–guest interactions,[3] rather than a continuum of states from which a potential guest can "sample" (Figure 1A and B). The question we pose here concerns whether it would be possible to create in one material a pore environment accessing an infinite number of energy states. Here, we use multivariate (MTV) strategy,[4] by which multiple functional groups can be introduced into one metal–organic framework (MOF) crystal without altering the underlying topology. In this study, three organic linkers bearing three different functional groups are incorporated into one metal–organic framework structure, and they do so using multiple ratios of those functional groups were used to produce pores endowed by multivariable functionalities. This allows for the access of a continuum of energy states that fit between the existing discrete energy levels given by the pristine MOFs, thus tuning the release profile of guest molecules in a precise manner and over a wide range (Figure 1C).

Specifically, we used the well-known MOF, MIL-101(Fe),[5] composed of Fe_3O SBUs and benzene dicarboxylate (BDC) linkers, to construct multivariate MOFs (MTV-MOFs) with the functional groups of $-H$, $-NH_2$, and $-C_4H_4$, MIL-101(Fe)-$(NH_2)_x$, MIL-101(Fe)-$(C_4H_4)_x$, and MIL-101(Fe)-$(C_4H_4)_x(NH_2)_{1-x}$, where x is continuously varied between 0 and 1 (Figure 2A). We subjected these MOFs to a set of three molecular guests [ibuprofen (Ibu), rhodamine B (RhB), and doxorubicin (DOX)] as probes in sampling the interior of these MOFs. We find that by varying the linker ratios in one MTV-MOF, (1) the release rate (r) of the probe molecules can be finely tuned between 0.30 and 1.14 d^{-1} (Ibu), 0.005 and 0.16 d^{-1} (RhB), 0.008 and 0.022 d^{-1} (DOX), (2) the time of maximum guest release can be programmed between 17 and 29 days (DOX), and (3) the corelease of guest probe molecules can be accomplished, in which the suppression or enhancement is in good accordance with the release of the single guest molecule. Furthermore, we used these results to develop a simple model to represent the host–guest interaction in terms of energy that can be precisely dialed-in, making it possible to predict the guest release kinetics for any specific linker ratio chosen from the continuum of MTV-MOFs. The power of this approach is revealed by the fact that such control cannot be

Received: July 15, 2017
Published: September 12, 2017

DOI: 10.1021/jacs.7b07392
J. Am. Chem. Soc. 2017, 139, 14209–14216

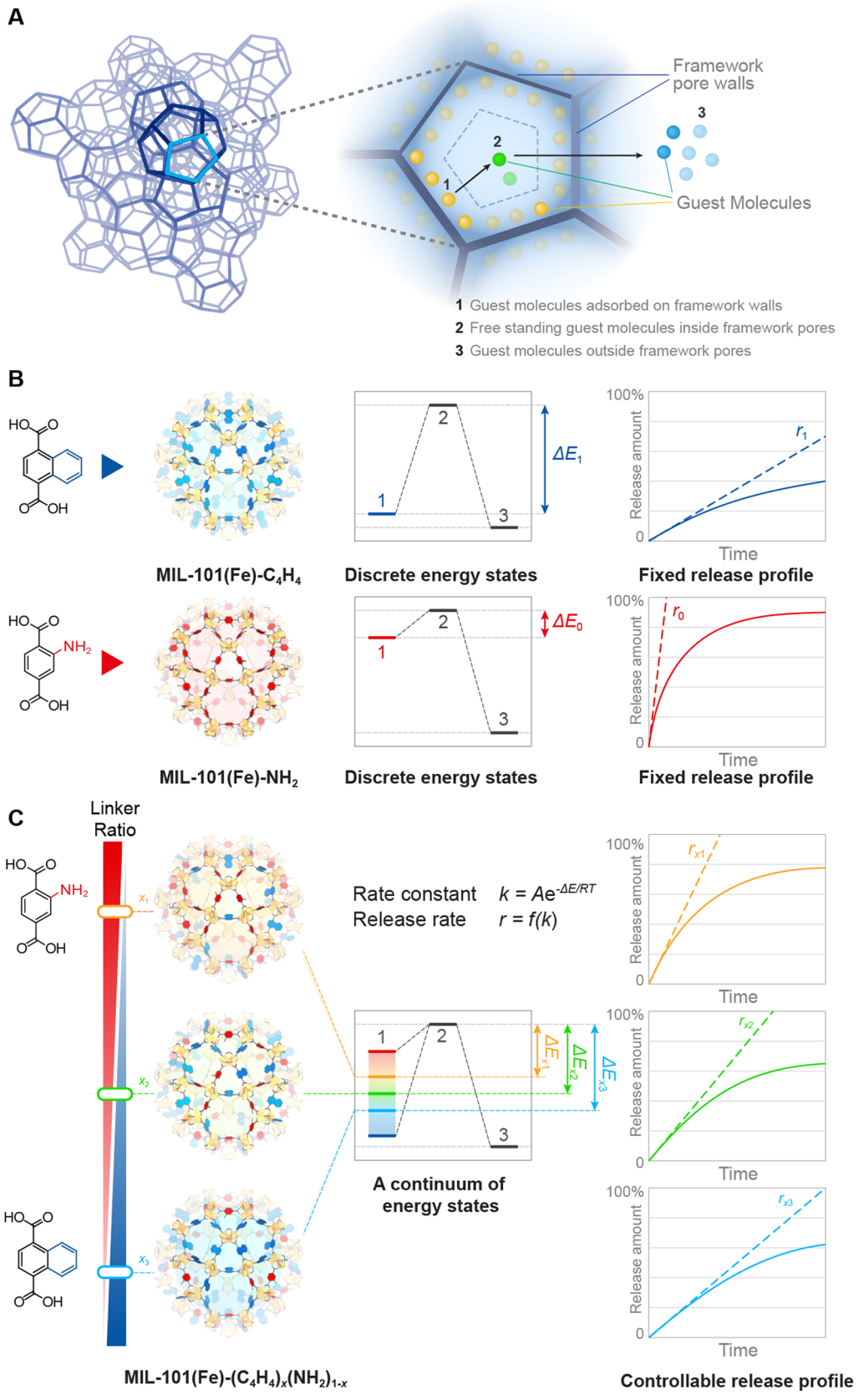

Figure 1. Comparison of MTV-MOFs with their single-component counterparts in the binding energy states and the guest molecules release profiles. (A) The release process of guest molecules from porous frameworks through three energy states. (B) Single-component MOFs provide discrete energy states representing specific interaction with guest molecules. This leads to fixed release profiles. (C) MTV-MOFs with various linker ratios present a series of continuous energy states from which guest release kinetics can be dialed-in over a wide range.

DOI: 10.1021/jacs.7b07392
J. Am. Chem. Soc. 2017, 139, 14209−14216

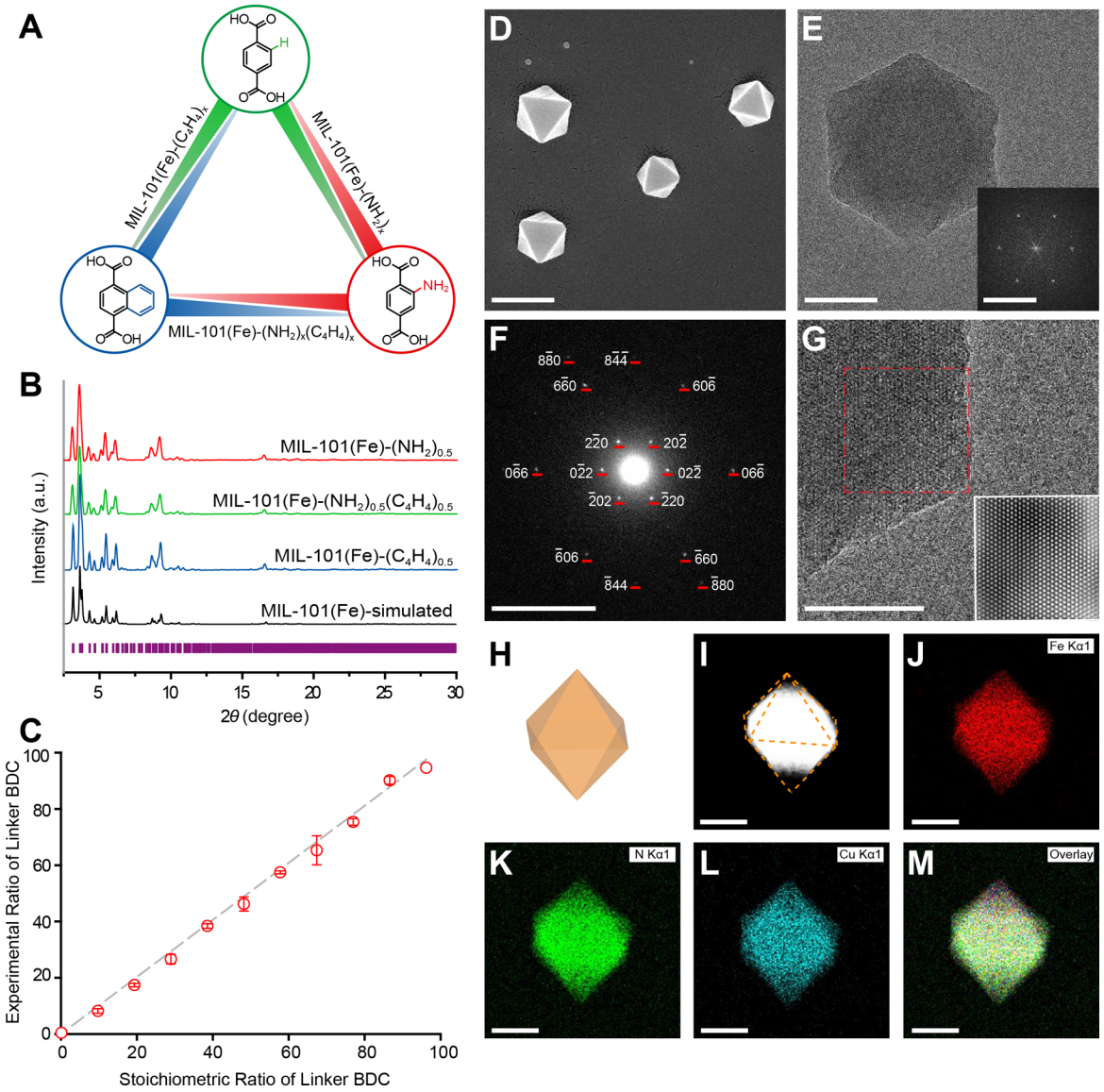

Figure 2. Structural and compositional characterizations of MTV-MIL-101(Fe) materials. (A) The combinations of multiple organic linkers in MTV-MIL-101(Fe) series. (B) Powder XRD patterns of MTV-MIL-101(Fe) samples matched well with the pristine MOF structure. (C) The plot of experimental linker ratio determined by ^{1}H NMR versus stoichiometric feeding ratio in MIL-101(Fe)-$(C_4H_4)_x(NH_2)_{1-x}$ reveals a linear relationship. (D–F) SEM image, TEM image, and electron diffraction pattern of MIL-101(Fe)-$(C_4H_4)_{0.5}(NH_2)_{0.5}$ single crystals, respectively (inset: fast Fourier transformation of the image). (G) HRTEM image shows the hexagonal pore arrangement (inset: the inverse fast Fourier transformation of the selected area). (H,I) Illustration and STEM images of MIL-101 framework, respectively. (J–M) EDS mapping of Fe, N, Cu elements and their overlay images of MIL-101(Fe)-$(C_4H_4)_{0.5}(NH_2)_{0.5}$ sample, respectively. Scale bar is 500 nm in (D), 100 nm in (E), 5 nm^{-1} in inset of (E), 10 nm^{-1} in (F), and 200 nm in (I–M).

achieved by a physical mixture representing those mixed linker ratios or in other porous materials.

Among vast uses of MOFs, attention has been drawn recently to their biomedical applications, such as drug delivery and photodynamic therapy.[6] Unlike other materials where the release of guest molecule relies on structure decomposition or outside stimuli, in this study, the release from MTV-MOFs is mainly driven by diffusion. Two of our probe molecules (Ibu and DOX) are commercialized drugs. By precisely dialing-in the host–guest interaction between MOFs and each drug molecule, their release rate can be seamlessly tuned, the time to reach release peak can be shifted, and their corelease can be precisely programmed. The three unique properties above originate from the intrinsic structural feature of MTV-MOFs. These materials and this approach add in efforts to further reveal the potentials of MOFs for drug release systems.

EXPERIMENTAL SECTION

General Synthetic Procedure of MTV-MOFs. Crystals of multivariate MIL-101(Fe) compounds were synthesized by mixing different linkers (Figure 2A) of various stoichiometry and ferric trichloride in dimethylformaldehyde (DMF) at 110 °C for 24 h.[5a,7] The as-synthesized MOF crystals were sequentially refluxed in DMF and ethanol using a Soxhlet extractor followed by evacuation under dynamic vacuum to prepare activated MOFs. The powder X-ray diffraction (PXRD) patterns were performed on a Rigaku Smartlab 9 kW X-ray diffractometer at room temperature. The exact proportion of linkers in MTV-MOFs was obtained by ^{1}H NMR spectroscopy through digesting the activated MTV-MOFs. SEM, TEM and EDS mapping images were collected using Zeiss SIGMA at 5kV, JEOL

DOI: 10.1021/jacs.7b07392
J. Am. Chem. Soc. 2017, 139, 14209–14216

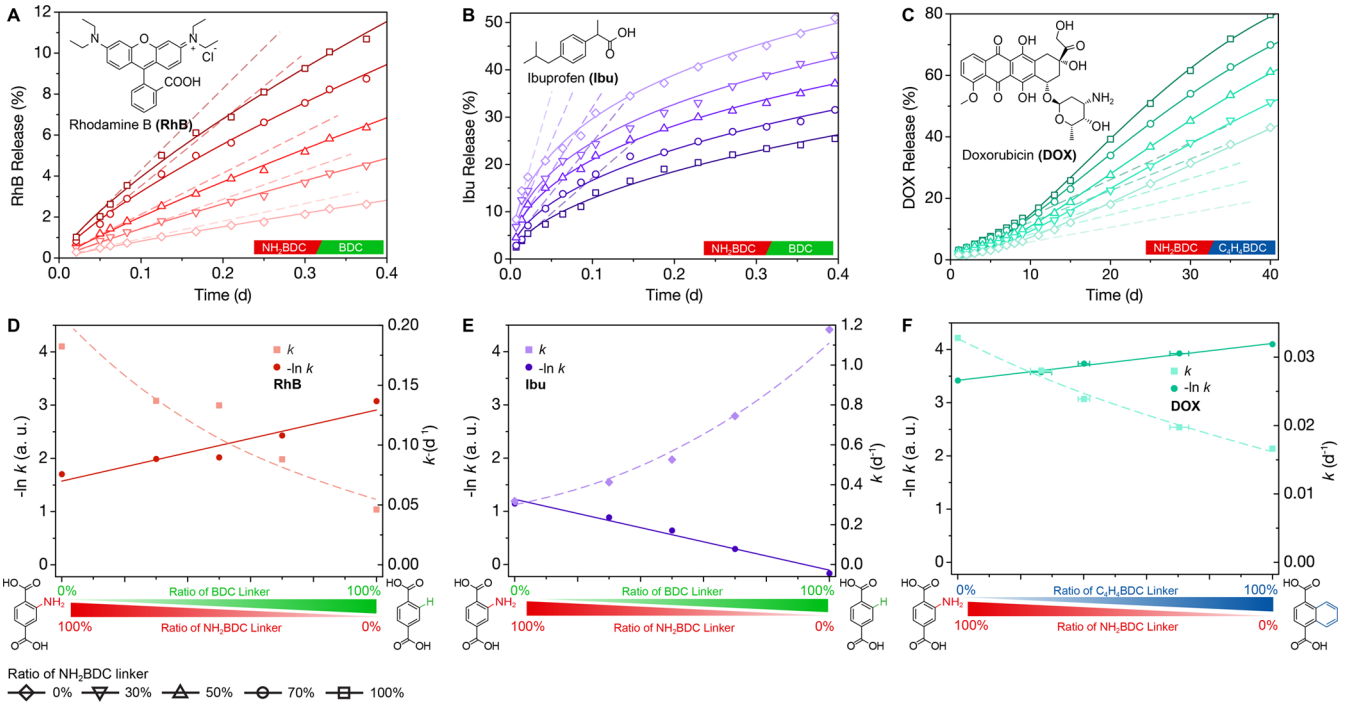

Figure 3. The fine-tuning of guest release kinetics, the correlation of host–guest interactions with functional groups. (A–C) Experimental (scatter dots) and fitted (curved lines) release kinetics of the probe molecules from multivariate MIL-101(Fe) samples as well as their initial release rates (dashed lines). (D–F) Relationship between release rate constants (k), $-\ln k$, and their correlation with the linker ratio in multivariate MIL-101(Fe) materials. The release of RhB from MIL-101(Fe)-$(NH_2)_x$ is described in (A) and (D), Ibu from MIL-101(Fe)-$(NH_2)_x$ in (B) and (E), and DOX from MIL-101(Fe)-$(NH_2)_x(C_4H_4)_{1-x}$ in (C) and (F), respectively. The arbitrary units in (D–F) are unified for clear comparison, the solid line represents the changes in $-\ln k$, and the dashed line represents the change in k.

JEM-2100 plus at 200kV and JEOL ARM-200F at 200 kV, respectively. After the guest molecules (Ibu, RhB, DOX) were loaded, the single/coloaded MOFs were put into dialysis bags and then suspended in 4-(2-hydroxyethyl)-1-piperazineethanesulfonic acid (HEPES) buffer to detect the release amounts. Detailed procedures and characterizations are provided in the Supporting Information.

Characterizations of MTV-MOFs. The structures of the MOFs do not decompose until 350 °C, as evidenced by thermal gravimetric analysis (TGA), indicating their high thermal stability and confirming full removal of solvent molecules from the pores (Figures S14–S21). Sharp peaks observed in PXRD patterns of the activated MTV-MOFs show that they are highly crystalline. The diffraction patterns matched well with the calculated pattern on the basis of the crystal structure of parent MIL-101 without any extra peaks, illustrating the phase purity of these MTV-MOFs (Figure 2B, Figures S2–S10). The permanent porosity of these MTV-MOFs is demonstrated by high uptake in the N_2 adsorption isotherms at 77 K. The Brunauer–Emmett–Teller (BET) surface areas of the MTV-MOFs, MIL-101(Fe)-$(NH_2)_{0.5}$, MIL-101(Fe)-$(C_4H_4)_{0.5}$, and MIL-101(Fe)-$(NH_2)_{0.5}(C_4H_4)_{0.5}$, are 2730, 3640, and 3420 $m^2\ g^{-1}$ (Table S2), respectively. All of these MOFs exhibit type IV isotherms, indicating the presence of mesopores (Figures S22–S45). The calculated pore size distribution using a nonlocal density functional theory (NL-DFT) model shows that two kinds of pores exist in MTV-MIL-101(Fe) (2.5 and 3.2 nm), which is consistent with the literature.[5] The linker ratios in the MTV-MOFs were quantitatively determined by ^1H NMR measurements of the digested MOF samples (Figures S11–S13). Unlike the bias observed in MTV-MOF-5 structures,[7b] a linear relationship between the stoichiometry of starting materials and actual linker ratios in the crystal structure was observed in the case of MTV-MIL-101 (Figure 2C). We attribute this to the mesoporosity of the MIL-101 structure, which minimizes linker–linker interactions. This linear relationship provides a precise control of the linker ratio in MTV-MIL-101(Fe) crystals.

The MTV-MIL-101(Fe) crystals exhibit octahedral morphologies in their scanning electron microscope (SEM) and transmission electron microscope (TEM) images (Figure 2D,E, Figures S46–S53), which are identical to those of the single component MOFs. High-resolution TEM (HRTEM) images of the MTV-MOF at [111] direction show pores in hexagonal arrangement, in good accordance with the pristine MOF structure (Figure 2E,G). Electron diffraction patterns at [111] direction further confirm that these octahedral particles are single crystals of the MTV-MOFs (Figure 2F). To show that various linkers are present in the MTV-MOF crystals, we used MIL-101(Fe)-$(NH_2)_{0.5}(C_4H_4)_{0.5}$ as an example, and postmodified the amino functional groups with 3-hydroxyphthalic anhydride to chelate Cu^{2+} so that the distribution of amino groups can be visualized under TEM by the Cu signal in the energy dispersive spectra (EDS) map (Figure 2I–M).[7a] The homogeneous distribution of N and Cu in a single crystal of this MTV-MOF illustrated the ubiquitous existence of BDC-NH_2 linker across the entire MOF structure. Multiple single crystals of the same MTV-MOF sample were examined, and the ratios of Cu to Fe were found to be the same, thus showing the homogeneity of bulk MTV-MOF samples (Figures S54 and S55, Table S3). MTV-MIL-101(Fe) crystals showed that all of the MOFs shared similar octahedral morphologies and particle sizes of about 300 nm (Figure 2D, Figures S46–S49). The consistency of all structural aspects of MTV-MOFs with varying linker ratios and those of the single-component counterparts rules out topological and morphological factors that might influence the interaction of these MOFs with guest molecules, which is crucial to correlate the host–guest interaction with their linker composition.

RESULTS AND DISCUSSION

Release Kinetics Analysis. Detailed studies of the interaction between MOFs and guest molecules were carried out by the loading and release of probe molecules. The loading of the probe molecules (RhB, Ibu, and DOX) into MTV-MOFs

DOI: 10.1021/jacs.7b07392
J. Am. Chem. Soc. 2017, 139, 14209–14216

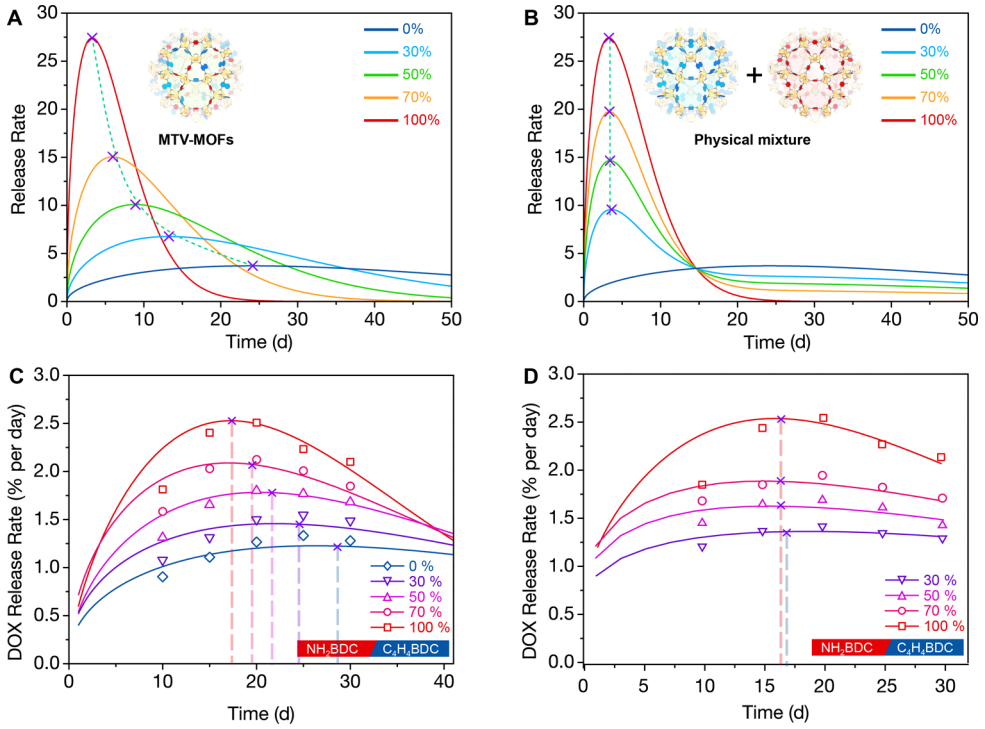

Figure 4. Program of the daily release amount in multivariate MOFs. The simulated daily release profiles of probe molecules from multivariate MOFs (A) and from the physical mixture of single-component counterparts (B) using the same set of energy parameters. Percentage of the linker that shows weaker interaction with the probe molecules is displayed. (C) The experimental daily release amount of DOX molecules from MIL-101(Fe)-$(C_4H_4)_x(NH_2)_{1-x}$ with different linker ratio. (D) The experimental daily release amount of DOX molecules from a physical mixture of the single-component MOF counterpart. Scatter dots are release amount average by the adjacent 3 days, and curve lines are the release rates derived from the fitted release profiles with a regression coefficient (r^2) of more than 0.99 to the experiment results.

and the single-component MOFs was achieved by immersion in saturated ethanol solutions of the probes. Subsequently, these MOFs were coated with anionic hyaluronic acid (HA) to further improve biocompatibility and enhance their stability in aqueous buffer solutions where the release experiments were performed. The TEM images reveal that a thin layer of HA with a thickness of around 20 nm was evenly deposited on the surface of the MOF particles, to ensure that the diffusion of probe molecules in and out of the MOFs remains unaffected (Figure S56). The MOFs loaded with probe molecules were put in a dialysis tube and then imbedded in a HEPES buffer solution for the release test. The amounts of guest molecules released were quantitatively monitored by HPLC in the case of Ibu and fluorescence spectra for RhB and DOX. The HA-coated MOF samples demonstrated exceptional stability as evidenced by their unaltered PXRD patterns after immersion in buffer solution over 18 days throughout the entire release process.

The guest release profiles of the probe molecules can be tuned by varying the ratio of organic linkers (Figure 3A–C and Figures S73–S79). In the case of the RhB release from the MIL-101(Fe)-$(NH_2)_x$ series, faster release is observed as the ratio of NH_2-BDC linkers increases, while the release slows when more BDC linkers are present (Figure 3A). In contrast, for MIL-101(Fe)-$(C_4H_4)_x$, the increase of BDC linker leads to faster RhB release, while the presence of C_4H_4-BDC linker slows the release process (Figure S74). It is clear that the functional groups in MTV-MOFs systems play an important role in interacting with probe molecules, thus controlling their release profiles. Stronger interactions between the functional groups and probe molecules will slow the release (such as $-C_4H_4$ to RhB), while weaker interaction will accelerate the process (such as $-NH_2$ to RhB). When combining two functional groups that interact strongly and weakly with the probe in one MTV-MOF, for example, in the case of the MIL-101(Fe)-$(NH_2)_x(C_4H_4)_{1-x}$ system, the release rates can be fine-tuned over a wide range up to 32-fold (Figure S75 and Table S6). In this way, we identified MTV-MOFs with the right type and proportion of functional groups, MIL-101(Fe)-$(NH_2)_{0.5}$, MIL-101(Fe)-$(C_4H_4)_{0.3}$, and MIL-101(Fe)-$(NH2)_{0.3}(C_4H_4)_{0.7}$, to achieve zero-order release, which is ideal for drug release systems.[8]

Host–Guest Interaction Analysis. The effect of functional groups also varies between different probe molecules. In the release of Ibu from MIL-101(Fe)-$(NH_2)_x$, the increase of NH_2-BDC linkers leads to slower release of Ibu, which is opposite to the accelerating tendency observed in the release of RhB from the same MTV-MOF under identical conditions (Figure 3B). In the case of DOX release, the effect of functional groups is similar to that of the RhB, where the $-NH_2$ group accelerates the release and the $-C_4H_4$ group slows the release (Figure 3C, Figures S79 and S84). On the basis of the results above, we conclude that there are strong correlations between functional groups and the release of probe molecules. This brings about the question: Is there any way to quantify such an interaction so that one can predict and program the release profiles of probe molecules?

To address this question, we derived a release kinetics model in the form of the cumulative distribution function, Weibull distribution,[9] based on the major interactions in host–guest systems (Figure 1, eq 1).

DOI: 10.1021/jacs.7b07392
J. Am. Chem. Soc. 2017, 139, 14209–14216

$$y = 1 - e^{-(kt)^n} \quad (1)$$

where y is the fraction of released guest molecules at time t, k is the release rate constant, which reflects host−guest interactions, and n is the guest−guest interaction parameter. We used this model to fit the experimental release curves of all three probe molecules in all MTV-MOF systems, and found that the fitted lines matched well with all of the experimental release curves (Figure 3A−C and Figures S85−S90) with a regression coefficient larger than 0.99. This model outperforms other common models in the fitting to the release behavior of all three probe molecules (Supporting Information section 6, Figures S95−S102), indicating that this model is appropriate for describing the release profiles in this study and correlating with the interaction in the probe release from MTV-MOFs systems. The interaction between the MOF and probe molecules can be derived using the Arrhenius equation to correlate the release rate constant (k), which is quantified by the Weibull model, with the energy state (E_a) that describes the host−guest interaction (Figure 1, eq 2).

$$k = A\, e^{-E_a/RT} \quad (2)$$

E_a represents the host−guest interaction energy as an activation energy, that is, the energy difference between the transition state and the reactant molecule, which are adsorbed guest molecules in the framework and free-standing guest molecules encapsulated in the pores, respectively (Figure 1A).[10] The negative natural logarithm of the rate parameter has a direct linear relationship with the interaction energy (eq 3).

$$-\ln k = \frac{E_a}{RT} - \ln A = \frac{E - E^*}{RT} \quad (3)$$

E is the energy presenting interaction between the probe molecules with MOF structure, and E^* is a reference state with $k = 1\ d^{-1}$. We investigated the rate constant k of the probe molecules releasing from a series of MTV-MOFs with various linker ratios and plotted it along with the $-\ln k$ against each ratio (Figure 3D−F). A linear relationship was observed. We also noticed the value of the guest−guest interaction parameter, n, remains nearly constant when the linker ratio varies in the same MTV-MOF system (Figure S91b and d). This allows us to calculate the $-\ln k$ value of a given linker ratio from the weighted average of the ratio and the host−guest interaction (here, represented by $-\ln k$) of the single-component MOF, and, subsequently, to predict release profiles of probe molecules for the MTV-MOF. We found that for all three probes, Ibu, RhB, and DOX, the predicted release profiles are in good agreement with the experimental results (Figures S92, 93b, and 94b). This demonstrates the validity of this model, and corroborates that it can be used to obtain the desired guest release kinetics by simply dialing-in the linker ratio of a selected MTV-MOFs. Moreover, in light of the fact that the value of host−guest interaction energy could be varied continuously, for the first time, we can access infinite and continuous energy levels as opposed to discrete states.

Because the release profile of a given probe can be predicted, the rate of release and increment of the daily release amount can be derived. In the case of DOX, the release rate increases from the beginning and, after a certain period, reaches a peak value before it starts to decline. By varying the linker combination and the ratio of the MTV-MOF, the time for the release to reach the peak can be tuned as shown in Figure 4A,C. This is in good accordance with the predicted trend using the release model of guest molecules (Figure 4A). In contrast, when using the physical mixture of two single-component MOFs with an identical ratio to the MTV-MOF, two peaks were observed, and the variation of mixture ratio adjusts the relative intensities of the peaks rather than shifts the peak position (Figure 4B,D). We simulated the release profile for the MTV-MOF system and the physical mixture separately, and found that indeed the programmable release of probe molecules can only be achieved in MTV-MOF systems (Figure 4A,B). The reason is that the pore environment is precisely controlled on the atomic scale by the presence of different functional groups in one MTV-MOF system, thereby directly tuning the interaction that each probe molecule can "sample" in the pores. This is reflected by the fine-adjustment of the $-\ln k$ value in the release model (Figure 3D−F). In contrast, the probe molecules experience different pore environments in physical mixtures of two separate MOFs, resulting in two distinct $-\ln k$ values and reflect by two peaks with the unchanged positions in the daily release profiles (Figure 4B,D). This experiment addresses the importance and uniqueness of the multivariate strategy, and further confirms the presence of multiple linkers as well as their well-mixed apportionment in one MTV-MOF crystal. It is worth noting that by dialing-in the host−guest interaction over a continuous range, the time to achieve the maximum release amount was shifted by 12 days, from the 17th to the 29th day in the case of DOX release from MIL-101(Fe)-$(NH_2)_x(C_4H_4)_{1-x}$ over a 40-day release period (Figure 4C). Such flexibility is not observed in the physical mixture of the single-component MOF counterparts (Figure 4B,D), and is previously inaccessible using other materials for the release of DOX molecules (Table S9).

Programmable Probes Release. The programmability is not only manifested in the controlled release of single probe molecules, but also in the corelease of multiple distinct probes. We tested the concurrent release of two sets of probes (RhB/Ibu and DOX/Ibu) in MIL-101(Fe)-$(NH_2)_x(C_4H_4)_{1-x}$ (Figure 5), and found that the trends of guest release are highly consistent with the aforementioned results from the release of single-loaded probes (Figure 5C and Figures S81−S84). In DOX/Ibu corelease systems, for example, the presence of more NH_2−BDC linkers that interact strongly with Ibu leads to the suppression of Ibu release; simultaneously, the presence of less C_4H_4-BDC linkers, which interact strongly with DOX, results in the promotion of DOX release in the same MTV-MOF (Figure 5C). These observations are in good agreement with the release profiles predicted by the model derived from the single-loaded probe release profiles. Brownian motion allows each probe molecule to "sample" the entire pore environment throughout the framework and experience all kinds of interactions (between probe and various functional groups, among probes of the same kind, and between different probes, Figure 5A). The test of single probe release allows us to screen various functional groups in the linkers and identify one that can pair up with the probe through a dominant interaction, reflected in large $-\ln k$ values, such as NH_2-BDC to Ibu and C_4H_4-BDC to DOX (Figure 5B). In this way, the behavior of each probe in corelease systems can be directed by dialing-in the exact ratio of the paired-up functional groups in MTV-MOFs (Figure 5A, SI section 4). The establishment of a clear correlation between functional groups and guest molecules provides a potential way to design carrier materials for programmed release of multiple drugs.

DOI: 10.1021/jacs.7b07392
J. Am. Chem. Soc. 2017, 139, 14209−14216

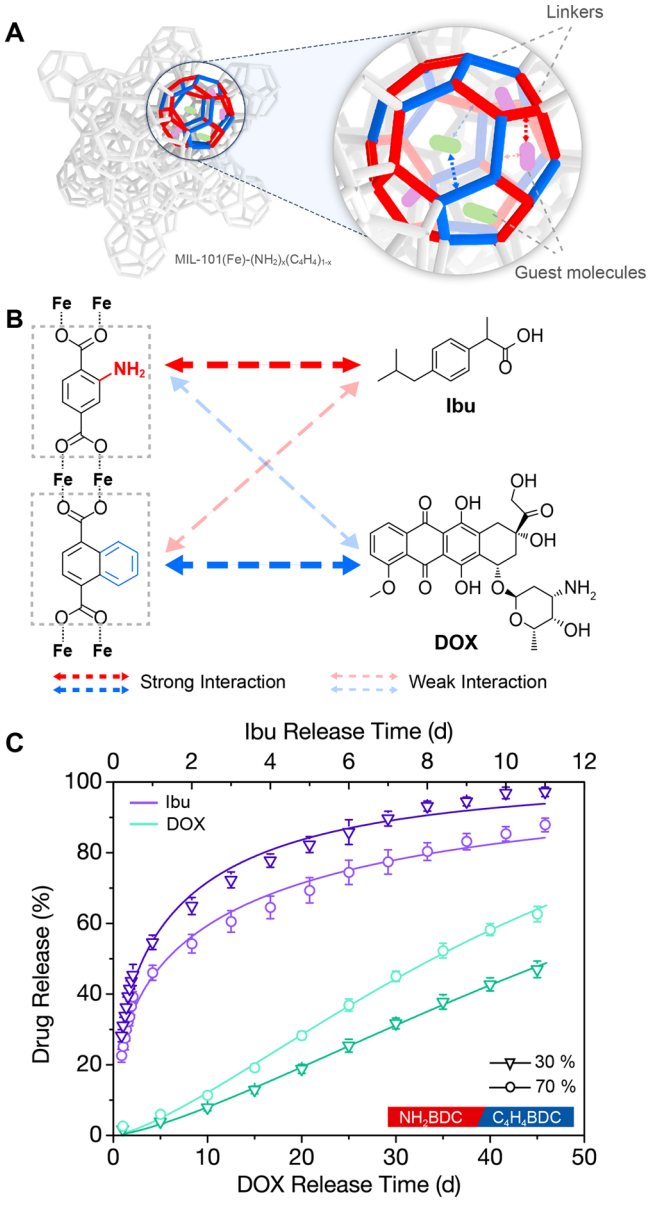

Figure 5. Programming the release profile of guest molecules through tuning the proportion of functional groups. (A) Illustration of pore environment "sampled" by two kinds of guest molecules. (B) Guest molecules and functional groups paired up by strong interactions. (C) The corelease profiles of Ibu and DOX in MIL-101(Fe)-$(NH_2)_x(C_4H_4)_{1-x}$.

■ ASSOCIATED CONTENT

Supporting Information

The Supporting Information is available free of charge on the ACS Publications website at DOI: 10.1021/jacs.7b07392.

Synthesis and characterizations of MTV-MOFs, electron microscopy and elemental analysis, uptake of guest molecules as probes, release profiles of guest molecules from MTV-MOFs, quantification and prediction of the interaction between MOFs and guest molecules, comparison of different release models, biocompatibility analysis of MOFs and molecule delivery into cells, and additional references (PDF)

■ AUTHOR INFORMATION

Corresponding Author

*hdeng@whu.edu.cn

ORCID

Zhiyue Dong: 0000-0003-1160-3256

Hexiang Deng: 0000-0002-9398-7996

Notes

The authors declare no competing financial interest.

■ ACKNOWLEDGMENTS

The research was supported by the Natural Science Foundation of Jiangsu Province of China (BK20140410) and Nanotechnology Foundation of Suzhou City of China (ZXG201446), the National Key Basic Research Program of China (2014CB239203), Key Program of Hubei Provence (2015CFA126), and the Innovation Team of Wuhan University (2042017kf0232). We thank the Large-scale Instrument and Equipment Sharing Foundation and Core Research Facilities of Wuhan University and Wuhan National Laboratory for Optoelectronics (WNLO) for providing technical support, and beamline BL14B1 (Shanghai Synchrotron Radiation Facility) for providing the beam time and help during the experiments. We also thank P. Liu, X. Han (Shanghai Jiao Tong University), Y. Ma (ShanghaiTech University), H. Cong, S. Chen, N. Ma, X. Wang, Y. Guo, Q. Liu, X. Xu, and F. Ke (Wuhan University) for their invaluable assistance and discussion.

■ REFERENCES

(1) (a) Vantomme, G.; Jiang, S.; Lehn, J. M. *J. Am. Chem. Soc.* **2014**, *136*, 9509. (b) Houk, K. N.; Leach, A. G.; Kim, S. P.; Zhang, X. *Angew. Chem., Int. Ed.* **2003**, *42*, 4872. (c) Perez-Estrada, S.; Rodríguez-Molina, B.; Xiao, L.; Santillan, R.; Jiénez-Osés, G.; Houk, K. N.; Garcia-Garibay, M. A. *J. Am. Chem. Soc.* **2015**, *137*, 2175. (d) Deng, H.; Olson, M. A.; Stoddart, J. F.; Yaghi, O. M. *Nat. Chem.* **2010**, *2*, 439.

(2) (a) An, J.; Geib, S. J.; Rosi, N. L. *J. Am. Chem. Soc.* **2009**, *131*, 8376. (b) Chandler, B. D.; Enright, G. D.; Udachin, K. A.; Pawsey, S.; Ripmeester, J. A.; Crame, D. T.; Shimizu, G. K. H. *Nat. Mater.* **2008**, *7*, 229. (c) Kim, S. H.; Shum, H. C.; Kim, J. W.; Cho, J. C.; Weitz, D. A. *J. Am. Chem. Soc.* **2011**, *133*, 15165. (d) Li, X.; Zhou, L.; El-Toin, A. M.; Zhang, F.; Zhao, D. Y. *J. Am. Chem. Soc.* **2014**, *136*, 15086. (e) Liong, M.; Angelos, S.; Choi, E.; Patel, K.; Stoddatrt, J. F.; Zink, J. I. *J. Mater. Chem.* **2009**, *19*, 6251.

(3) (a) Matsuzaki, S.; Arai, T.; Ikemoto, K.; Inokuma, Y.; Fujita, M. *J. Am. Chem. Soc.* **2014**, *136*, 17899. (b) Snyder, M. A.; Vlachos, D. G. *Phys. Rev. E* **2005**, *71*, 060201R.

(4) (a) Henke, S.; Schneemann, A.; Wütscher, A.; Fischer, R. A. *J. Am. Chem. Soc.* **2012**, *134*, 9464. (b) Li, Q.; Zhang, W.; Miljanić, O. Š.; Sue, C.-H.; Zhao, Y.-L.; Liu, L.; Knobler, C. B.; Stoddart, F.; Yaghi, O. M. *Science* **2009**, *325*, 885. (c) Wilmer, C. E.; Leaf, M.; Lee, C. Y.; Farha, O. K.; Hauser, B. G.; Hupp, J. T.; Snurr, R. Q. *Nat. Chem.* **2012**, *4*, 83. (d) Falcaro, P.; Okada, K.; Hara, T.; Ikigaki, K.; Tokudome, Y.; Thornton, A. W.; Hill, A. J.; Williams, T.; Doonan, C.; Takahashi, M. *Nat. Mater.* **2017**, *16*, 342. (e) Helal, A.; Yamani, Z. H.; Cordova, K. E.; Yaghi, O. M. *Nat. Sci. Rev.* **2017**, *4*, 296. (f) Popp, T. M. O.; Yaghi, O. M. *Acc. Chem. Res.* **2017**, *50*, 532.

(5) (a) Bauer, S.; Serre, C.; Devic, T.; Horcajada, P.; Marrot, J.; Férey, G.; Stock, N. *Inorg. Chem.* **2008**, *47*, 7568. (b) Férey, G.; Mellot-Draznieks, C.; Serre, C.; Millange, F.; Dutour, J.; Surblé, S.; Margiolaki, I. *Science* **2005**, *309*, 2040.

(6) (a) Lismont, M.; Dreesen, L.; Wuttke, S. *Adv. Funct. Mater.* **2017**, *27*, 1606314. (b) Wuttke, S.; Lismont, M.; Escudero, A.; Rungtaweecoranit, B.; Parak, W. J. *Biomaterials* **2017**, *123*, 172. (c) He, C.; Liu, D.; Lin, W.-B. *Chem. Rev.* **2015**, *115*, 11079. (d) Diring, S.; Carné-Sánchez, A.; Zhang, J.; Ikemura, S.; Kim, C.;

DOI: 10.1021/jacs.7b07392
J. Am. Chem. Soc. 2017, 139, 14209−14216

Inaba, S.; Kitagawa, S.; Furukawa, S. *Chem. Sci.* **2017**, *8*, 2381. (e) Teplensky, M. H.; Fantham, M.; Li, P.; Wang, T. C.; Mehta, J. P.; Young, L. J.; Moghadam, P. Z.; Hupp, J. T.; Farha, O. K.; Kaminski, C. F.; Fairen-Jimenez, D. *J. Am. Chem. Soc.* **2017**, *139*, 7522. (f) Horcajasier, P.; Gref, R.; Baati, T.; Allan, P. K.; Maurin, G.; Couvreur, P.; Férey, G.; Morris, R. E.; Serre, C. *Chem. Rev.* **2012**, *112*, 1232.

(7) (a) Garibay, S. J.; Wang, Z.; Tanabe, K. K.; Cohen, S. M. *Inorg. Chem.* **2009**, *48*, 7341. (b) Deng, H.; Doonan, C. J.; Furukawa, H.; Ferreira, R. B.; Towne, J.; Knobler, C. B.; Wang, B.; Yaghi, O. M. *Science* **2010**, *327*, 846. (c) Yuan, S.; Chen, Y.-P.; Qin, J.-S.; Lu, W.; Zou, L.; Zhang, Q.; Wang, X.; Sun, X.; Zhou, H.-C. *J. Am. Chem. Soc.* **2016**, *138*, 8912. (d) Aguirre-Díaz, L. M.; Gándara, F. M.; Snejko, N.; Gutiérrez-Puebla, E.; Monge, M. Á. *J. Am. Chem. Soc.* **2015**, *137*, 6132. (e) Burrows, A. D. *CrystEngComm* **2011**, *13*, 3623. (f) Kong, X.; Deng, H.; Yan, F.; Kim, J.; Swisher, J. A.; Smit, B.; Yaghi, O. M.; Reimer, J. A. *Science* **2013**, *341*, 882.

(8) (a) Lázaro, I. A.; Haddad, S.; Sacca; Orellana-Tavra, C.; Fairen-Jimenez, D.; Forgan, R. S. *Chem.* **2017**, *2*, 561. (b) He, C.; Lu, K.; Liu, D.; Lin, W.-B. *J. Am. Chem. Soc.* **2014**, *136*, 5181.

(9) Christensen, F. N.; Hansen, F. Y.; Bechgaard, H. *J. Pharm. Pharmacol.* **1980**, *32*, 580.

(10) Mitran, R. A.; Matei, C.; Berger, D. *J. Phys. Chem. C* **2016**, *120*, 29202.

DOI: 10.1021/jacs.7b07392
J. Am. Chem. Soc. 2017, 139, 14209−14216